

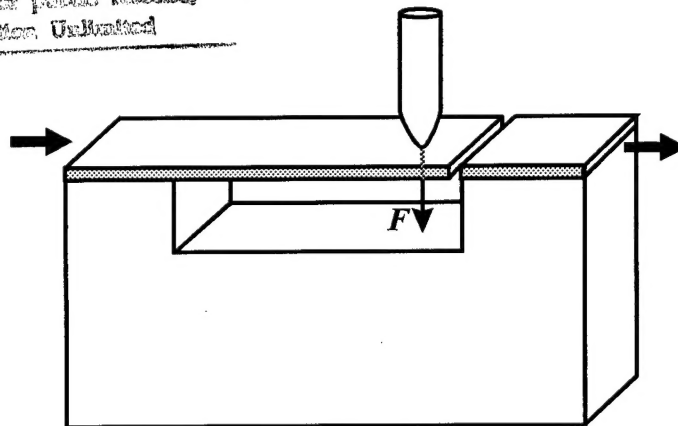
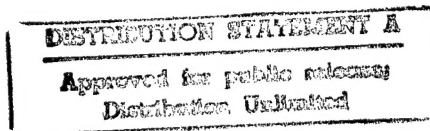
MOSCOW INSTITUTE OF PHYSICS AND TECHNOLOGY.  
Dolgoprudny, Moscow Region, 141700, Russia.

## Final Report

### SILICON MICROMECHANICAL OPTICAL WAVEGUIDE FOR MODULATION AND SENSING.

(Contract No. SPC-93-4048)

Principal Investigator:  
Dr. A.V.Churenkov.



19980316 097

DTIC QUALITY INSPECTED 3

12 October 1995

**REPORT DOCUMENTATION PAGE**

Form Approved OMB No. 0704-0188

Public reporting burden for this collection of information is estimated to average 1 hour per response, including the time for reviewing instructions, searching existing data sources, gathering and maintaining the data needed, and completing and reviewing the collection of information. Send comments regarding this burden estimate or any other aspect of this collection of information, including suggestions for reducing this burden to Washington Headquarters Services, Directorate for Information Operations and Reports, 1215 Jefferson Davis Highway, Suite 1204, Arlington, VA 22202-4302, and to the Office of Management and Budget, Paperwork Reduction Project (0704-0188), Washington, DC 20503.

1. AGENCY USE ONLY (Leave blank)	2. REPORT DATE  12 October 1995	3. REPORT TYPE AND DATES COVERED  Final Report	
4. TITLE AND SUBTITLE  Silicon Micromechanical Optical Waveguide for Modulation and Sensing		5. FUNDING NUMBERS  F6170893W0754	
6. AUTHOR(S)  Dr. A.V. Churenkov		8. PERFORMING ORGANIZATION REPORT NUMBER  SPC-93-4048	
7. PERFORMING ORGANIZATION NAME(S) AND ADDRESS(ES)  Moscow Institute of Physics and Technology Dolgoprudny, Moscow Region 141700, Russia			
9. SPONSORING/MONITORING AGENCY NAME(S) AND ADDRESS(ES)  EOARD PSC 802 BOX 14 FPO 09499-0200		10. SPONSORING/MONITORING AGENCY REPORT NUMBER  SPC-93-4048	
11. SUPPLEMENTARY NOTES			
12a. DISTRIBUTION/AVAILABILITY STATEMENT  Approved for public release; distribution is unlimited.		12b. DISTRIBUTION CODE  A	
13. ABSTRACT (Maximum 200 words)  The microstructure, optical and mechanical properties of the silicon micromechanical optical waveguide are investigated. The physical principles of mechanical excitation of the cantilever waveguide by photothermal, magnetostriction, and by direct force action are considered. The sensor application of the developed device is analyzed.			
14. SUBJECT TERMS		15. NUMBER OF PAGES  20	
		16. PRICE CODE	
17. SECURITY CLASSIFICATION OF REPORT  UNCLASSIFIED	18. SECURITY CLASSIFICATION OF THIS PAGE  UNCLASSIFIED	19. SECURITY CLASSIFICATION OF ABSTRACT  UNCLASSIFIED	20. LIMITATION OF ABSTRACT  UL

NSN 7540-01-280-5500

Standard Form 298 (Rev. 2-89)  
Prescribed by ANSI Std. Z39-18  
298-102

## SILICON MICROMECHANICAL OPTICAL WAVEGUIDE FOR MODULATION AND SENSING.

*The results and conclusions of the project are summarized in the final report. The microstructure, optical and mechanical properties of the silicon micromechanical optical waveguide are investigated. The physical principles of mechanical excitation of the cantilever waveguide by photothermal, magnetostriction, and by direct force action are considered. The sensor application of the developed device is analyzed.*

### 1. INTRODUCTION

Recent trends in the scientific and engineering literature indicate a growing interest in the use of crystalline silicon as a material for guided-wave optics [1-6]. There are several reasons of economic and technical character that make it more attractive to utilize the Si-based opto-electronics in comparison with the one based on III-V semiconductor materials. First of all it is low cost of silicon as compared to III-V binary crystal materials. It has billions of dollars of development behind it for the implementation of economic mass production. As semiconductor it affords the opportunity of integrating into one piece both mechanical device and electronic circuit. Single-crystal silicon is suitable for low-loss waveguiding at the fiber-optical communications wavelength  $\lambda=1.3\ \mu\text{m}$  or  $\lambda=1.55\ \mu\text{m}$ . At these wavelengths silicon is exhibiting lower attenuation than lithium niobate widely utilized in integrated optics. Silicon can be anisotropically wet etched to produce highly accurate components [7,8]. The mechanical and thermal advantages of single-crystal silicon substrates are well known. Also, the silicon wafers are available in 8-inch diameters, a size not found in *InP* or *GaAs*. Silicon circuits have a tremendous knowledge-base and experience-base. The great maturity of silicon processing can be applied in many respects to silicon-based optics and electrooptics in order to move the new optical devices rapidly "up the learning curve". Thus, the development of micromechanical optical waveguides based on the single-crystal silicon is currently the actual research problem, the solution of which may lead to creation of a new family of devices of a big practical value.

This work is devoted to the development of silicon micromechanical waveguide for the purposes of light modulation/switching and for sensing of diverse environmental parameters such as force, acceleration, and other force-related parameters. The idea was to form a silicon waveguide by micromachining etching techniques into a suspended cantilever beam that can be deformed arousing the modulation of the light intensity. Such idea have been partially realized by other authors only for glass waveguides on the silicon substrate, while it is for the first time, when silicon micromechanical waveguide is demonstrated [9].

Several basic approaches to fabrication of the micromechanical waveguide were considered by us. We have chosen SOI (Silicon On Insulator) techniques assuring fairly low propagation losses and providing more reliable and consistent fabrication process as

compared to alternative  $n/n^+$  (or  $p/p^+$ ) technique. For modulation of the light intensity the cantilever suspension of the silicon waveguide has been used (Fig.1e). In this case the vertical deviation of the microcantilever gives rise to waveguide misalignment and to modulation of intensity of propagating light. In comparison with suspended microbeam such approach does not require utilization of the opto-elastic effect and interferometric detection technique and, therefore, more simple and reliable. Several microfabrication processes such as silicon wafer bonding, wet and vertical dry etching, etc. have been involved.

There are a number of means to excite oscillation in micromechanical waveguide or to deviate it, besides electrostatic excitation. It may be, for example, direct action of a rod, what is especially interesting for sensing of force or displacement. Photothermal excitation of waveguide vibrations allows to modulate the light by light. It is very promising also to utilize metallic glass coatings sputtered onto Si-waveguide. First, such coating may serve as a driving layer and, second, because of hysteresis can be utilized in optical elements of memory.

## 2. TECHNOLOGICAL ROUTE

The new technological route for the fabrication of the silicon micromechanical optical waveguide has been developed. The structure is designed as SOI waveguide with flexible section clamped as a cantilever (Fig.1e). The thickness of the waveguide layer is about  $10\mu$ , while the thickness of the oxide buffer layer is about  $1\mu$ . Deviations of the cantilever result in waveguide misalignment and lead consequently to optical modulation. The essence of the new method developed by us is two-side photolithography on the bonded and thinned wafers (below the thinned wafer is referred to as the seed wafer, while the wafer with the rectangular pits is called the handle wafer). Both the anisotropic wet etching and dry ion beam etching were used for fabrication of the cantilever waveguide over the rectangular pit. The process of microfabrication consists of the following steps :

1. Lapping and polishing of both the handle and the seed wafer. Oxidation of the handle wafer by pyrolytic method (Fig. 1a).
2. Bonding the seed and handle wafers by method of thermocompressive direct silicon bonding (Fig. 1b).
3. Thinning the seed wafer with lapper/polisher till the thickness of about 10 micrometers (Fig. 1c).
4. Polishing of the bottom side of the handle wafer for two sides photolithography.
5. Photolithography and anisotropic wet etching of rectangular pits from the bottom side of the handle wafer (Fig. 1d).
6. Coating of the top side surface of the seed wafer by *Cr*.
7. Photolithography on the seed wafer with infra-red microscope and dry plasma etching of the seed wafer with formation of the silicon cantilever (Fig. 1e).
8. Breaking the wafer into the separate micromodulator chips.

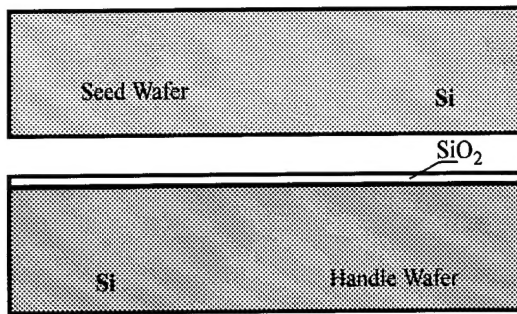


**Fig. 1a.** Polishing of seed and handle wafers.  
Oxidation of the handle wafer.

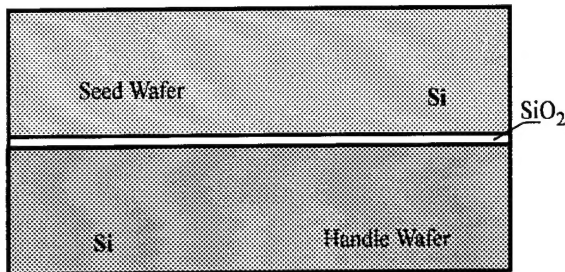


**Fig. 1b.** Direct silicon bonding of the seed and the handle wafers.

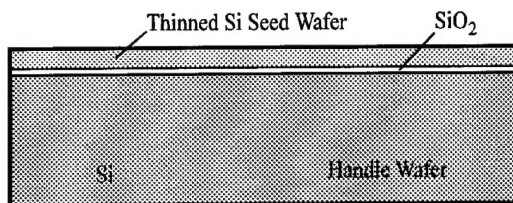


**Fig. 1c.** Thinning of the bonded wafers

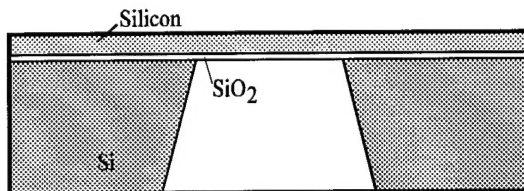


**Fig. 1d.** Anisotropic wet etching from the bottom side of the handle wafer

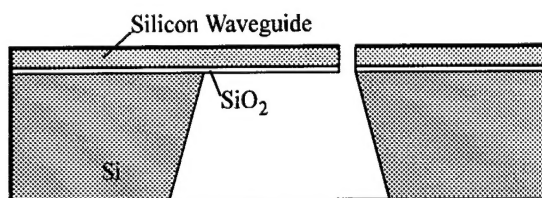


**Fig. 1e.** The silicon micromechanical optical waveguide formed as a result of the dry plasma etching from the top side of the seed wafer

### 3. PECULIARITIES OF MICROFABRICATION PROCESS

#### 3.1. Silicon wafers and oxidation.

Two silicon wafers were used in the process of microfabrication. Both wafers were of  $\langle 111 \rangle$ -type. To diminish the light attenuation by free carriers in silicon, the seed wafer was only slightly doped by phosphorus with  $\rho = 10 - 20 \Omega \cdot \text{cm}$ , so it was n-type wafer with dopant density  $N$  less than  $10^{15} \text{cm}^{-3}$ . The surface of this wafer was highly polished mechanically and treated then chemically. As a result its surface got a hydrophilous properties.

The handle wafer was of 76 mm (3") diameter, highly doped. The top side of this wafer was preliminary polished and then an oxide layer of  $1 \mu\text{m}$  thick was deposited onto this surface by pirolytic method. Utilization a high-temperature oxidation is more power-consumption method in this case and therefore it is more expensive. For this reason pirolytic method has been chosen.

#### 3.2. Silicon Direct Bonding (SDB).

A new technique developed by us was used during SDB [10]. The method is based upon the phenomenon of semiadhesion of silicon surfaces at the room temperature and realized in two stages: firstly, setting in contact hydrated silicon surfaces at the room temperature, and, secondly, thermal treatment of the monolithic multilayer junction. The presence of the silicon dioxide acting as an optical barrier between the seed and the handle wafers improves the quality of SDB. According to the opinion of many investigators the initial adhesion occurs mainly due to hydroxyl ion groups  $\text{OH}^-$  absorbed by the silicon surfaces. From the local regions the process of bonding is spread occupying almost all the area of contacted surfaces. Substituting the hydrogen ties for the silicone one with diffusion of generated water all over the surface of junction allows to form not only Si-Si structures with very thin natural oxide layer, but also  $\text{Si-SiO}_2\text{-Si}$  structures bonding silicon wafer directly with the silicon dioxide layer.

At the first stage carefully cleaned, brightly finished and chemically activated surfaces have to be used. At the second stage high temperature treatment ( $T = 1200^\circ\text{C}$ , 30 minutes) with applying a compressive stress is used. Both stages are fulfilled with the use of a special designed quartz cassette. Before setting into the cassette the wafers are treated by a special chemical composition, cleaned in distillate water, and then dried in the centrifuge. As a result of SDB the structure consisted of two bonded wafers was formed (Fig.1b).

During the high-temperature stage of SDB an intensive diffusion between the outside silicon layers and internal  $\text{SiO}_2$  layer is occurred. As a result there will be no step configuration of refractive indexes at the border  $\text{Si-SiO}_2$ . This may change the mode composition of the light propagating by the waveguide.

### 3.3. Thinning of the seed wafer.

The bonded wafers are thinned to fabricate the upper silicon layer of necessary thickness (about 10  $\mu\text{m}$ ). The process was divided into several stages. On the first stage of thinning the rough lapping with the soft lapper was used. As a result of this stage the upper seed wafer is thinned to 50  $\mu\text{m}$ . On the following stages the chemical-dynamic polishing was used, which allows the thickness of 9-11  $\mu\text{m}$  to be achieved with brightly polished wafer surface. Three consequential polishing and measuring processes were required to achieve the necessary thickness. The main problem here is the nonuniformity of the polisher because of taper, bow, microrelief and variation of the pressure to the wafer. As a result, the thickness of the polished seed wafer is considerably changed from place to place and the partial removal of the upper layer was even observed. This certainly may cause the problems for the mass industrial production, so the thinning by the chemical means with an etch-stop seem to be more preferable method.

### 3.4. Wet etching of the handle wafer.

The rectangular pits were etched from the bottom side of the handle wafer. For this purposes the bottom side surface of the handle wafer was brightly polished and the standard

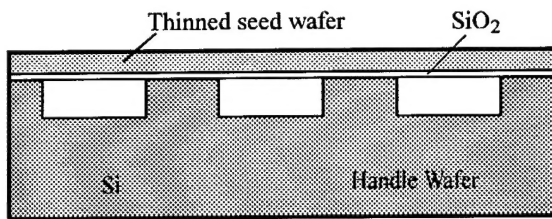


Fig. 2. The bonded wafers with the sealed pits.

photolithography process was fulfilled. There are several advantages of this technology. First of all, there is no necessity to control the depth of etching, because the process is stopped automatically as the pit bottom reaches the isolation  $\text{SiO}_2$  layer. Second, there are no sealed pits, where the excessive pressure may appear. Several experiments with such structures were done. The observation of the ready bonded and thinned wafers in the reflected light shows that the thinned seed wafer is really curved a bit over the square pits. The use of the through holes remove this problem.

### 3.5. High-depth ion-beam vertical dry etching.

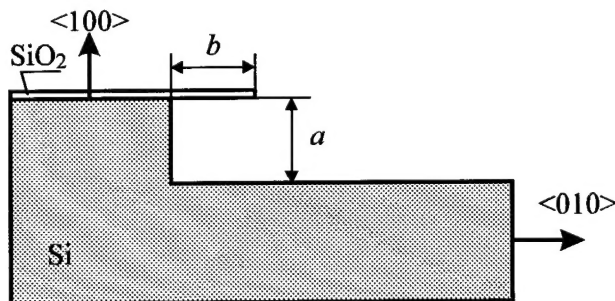


Fig.3. Vertical wet etching and undercutting in  $\langle 100 \rangle$  silicon wafer with  $\text{SiO}_2$  mask. The etch depth  $a$  equals undercutting  $b$ .

To diminish the attenuation of the light propagating by a silicon waveguide the narrow gap and vertical walls are required. Several silicon micromachining techniques allow the vertical etching to be fulfilled. First, this is the anisotropic wet



etching in  $\langle 100 \rangle$  silicon wafer [11]. In this case the boundary of the mask is aligned by such a way that perpendicular to it lays in  $\langle 010 \rangle$  direction. The etching rate in  $\langle 100 \rangle$  direction equals to undercutting rate. As a result, the vertical wall is fabricated (Fig.3). When the depth of etching is about  $10\text{ }\mu\text{m}$  (as in our case), the gap will be wider than  $25\text{ }\mu\text{m}$  and strong light dissipation occurs at the gap. Additionally, the roughness of the walls will increase the attenuation of the light in the waveguide.

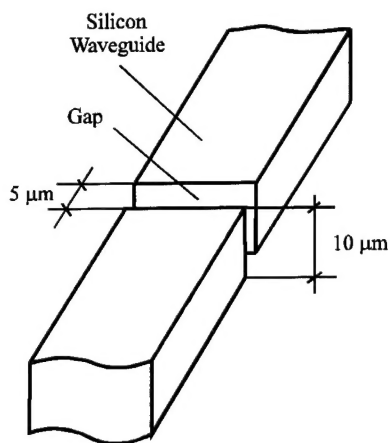


Fig.4. The silicon micromechanical optical waveguide with narrow gap.

For this reason we have considered an alternative method of vertical etching -- dry plasma etching. The main problem, which appears here, is high depth of etching. From the one side, this requires high survivability of the metallic mask and, from the other side, special efforts have to be applied to fabricate the vertical wall. When the depth of etching is about several micrometers, no difficulties with plasma etching arise. If we etch the wafer deeper than  $10\text{ }\mu\text{m}$ , the mask will be intensively etch off, while the wall may be oblique, or curved. Several metals were tested for a mask. Only *Cr* and *NiCr* were found to be acceptable for high-depth plasma etching, while *Al* and *Ni* masks were etched off. The shape of the walls was found to be strongly dependent upon the etch conditions: gas composition, temperature, etc.

Let us consider the experimental results in details. The depth of etching, mask undercutting, mask etch off, verticalness and shape of the walls were investigated. The narrow ( $5\text{ }\mu\text{m}$ ) and deep ( $10\text{--}15\text{ }\mu\text{m}$ ) gap between the silicon waveguides (Fig.4) proved to be most difficult problem of this stage. Our objective was to fabricate by dry ion etching a silicon waveguide suspended over a rectangular pit as cantilever with vertical and flat walls, small mask undercutting and etching off. As a result of these investigations the set-up acceptable for high-depth ion dry etching has

been developed and the necessary regimes have been found. The wall was practically vertical and flat. Only near the bottom of the waveguide the wall was found to be curved (Fig.5). The result of plasma etching was observed with the aid of electron microscope.

To fulfill the dry ion etching the top surface side of the seed wafer was coated by *Cr* layer. Then, the mask was aligned in the infra-red light with the aid of microscope. By such

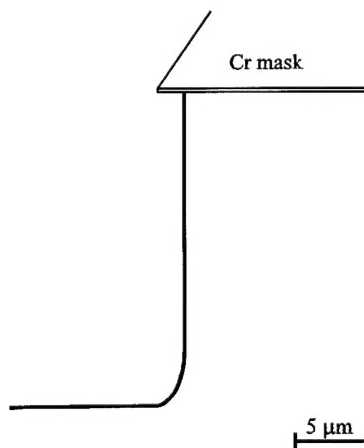


Fig.5. The wall of the waveguide fabricated by means of dry plasma etching.



a way the pits structure of the handle wafer was seen through the seed wafer, and the waveguide gaps were situated at the edge of the rectangles. The suspended cantilever waveguides were formed as a result of plasma etching from the side of the seed wafer.

### 3.6. Breaking the wafer into the separate chips.

Several micromodulator chips were fabricated in one silicon wafer. To separate this wafer into the several chips the special grooves were etched from the bottom side of the handle wafer (Fig.6). This allowed the micromodulator chips to be separated by breaking, and not cutting.

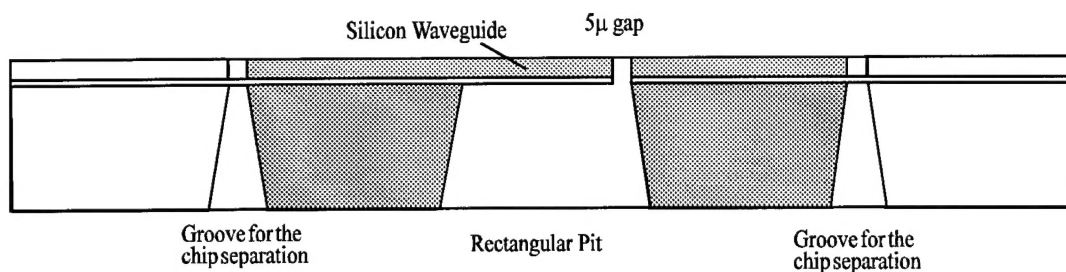


Fig.6. The fragment of the wafer with the grooves for the chips separation.

## 4. MICROSTRUCTURE, OPTICAL AND MECHANICAL TESTS.

### 4.1. MICROSTRUCTURE OF THE MODULATOR

The microstructure of the silicon micromechanical optical waveguide was investigated with the aid of electron microscope. Photo 1 shows the cantilever waveguide suspended over the rectangular pit. A narrow gap is seen in the Photo. The top surface of the cantilever waveguide is coated by *Cr* layer. The considerable roughness of the cantilever is seen in the Photo, which are the result of a strong mask etching-off. The cantilever beam was found to be curved a bit under the action of the compressive stress generated inside the mask layer during *Cr* deposition. When this mask is removed the bend disappears and two sections of the waveguide are aligned.

Strong mask etch-off was observed after the ion beam etching. Photo 2 shows the waveguide gap after the ion-beam etching (top view), photo 3 and 4 are the top-lateral view of the same gap. From the top side of the cantilever waveguide we can see the remainders of the *Cr* mask. In many places of the tested sample the mask was found to be etch-out, while the mask of many other samples was showed to be survived.

The regions of the cantilever waveguide, where the mask was etched-out, were tested in  $1\mu\text{m}$  layer for the presence of impurities. The results are shown in Fig.7 and Fig.8. Fig.7 shows the spectrum obtained with electron microscope. Several maximums are seen in the figure, which corresponds to different elements of impurities. Considerable amount of *Fe* was detected in thin top layer of the silicon waveguide (8%). The amount of *Cr* and

Al was found to be high as well. The percentage of other elements in 1 $\mu$ m surface layer are shown in Fig.8. Probably the strong diffusion of the metals took place during high-depth ion-beam etching. The pollution of the silicon waveguide can be diminished by diminishing of the etch depth and by choosing of the gas composition.

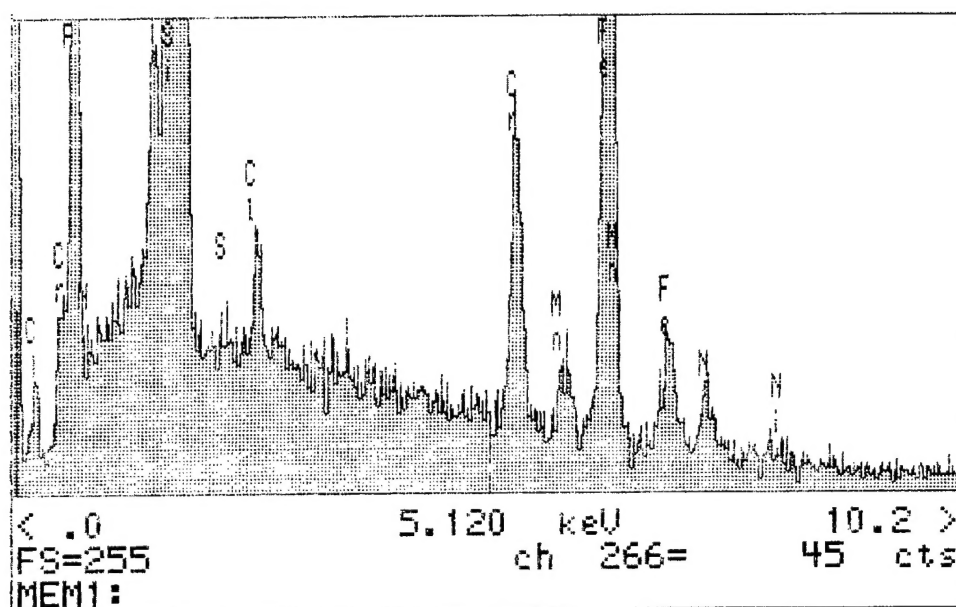
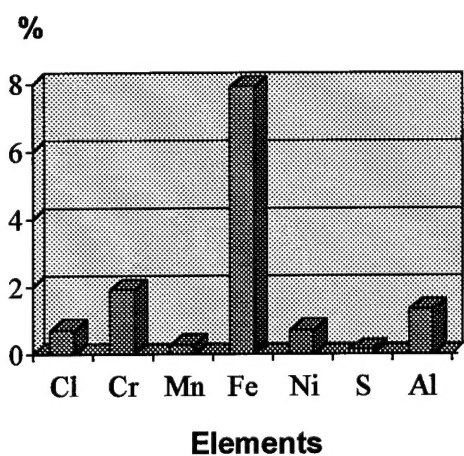
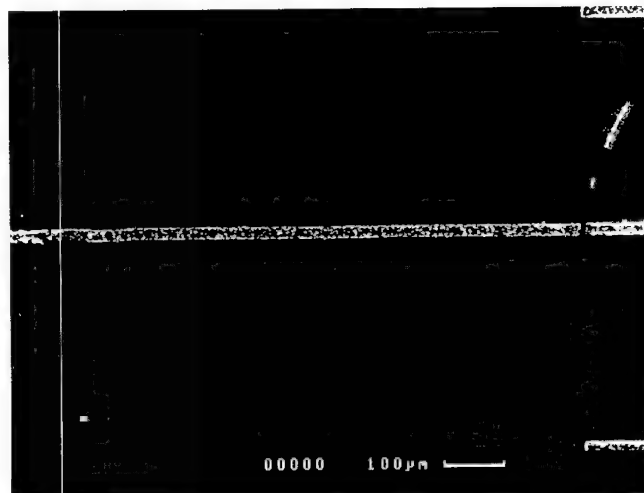


Fig.7. Impurities in the cantilever surface layer. Electron microscope spectrum.



Elements	%
Si	87.03
Cl	0.71
Cr	1.92
Mn	0.25
Fe	7.92
Ni	0.70
S	0.13
Al	1.33
Total	100%

Fig.8. The impurities in 1 $\mu$ m surface layer of the cantilever waveguide.



**Photo 1.** Silicon micromechanical optical waveguide suspended over the rectangular pit.  
The narrow gap is seen from the right side of the cantilever.

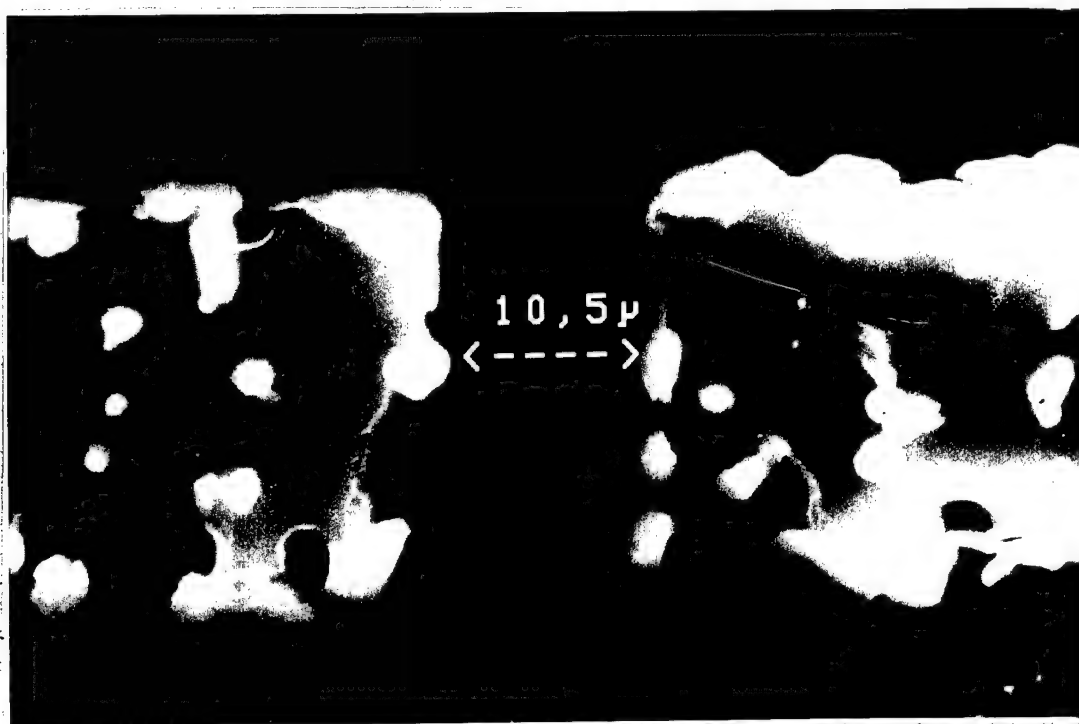


**Photo 2.** The gap between two sections of the silicon waveguide.  
White spots are the remainder of Cr mask. Top view.

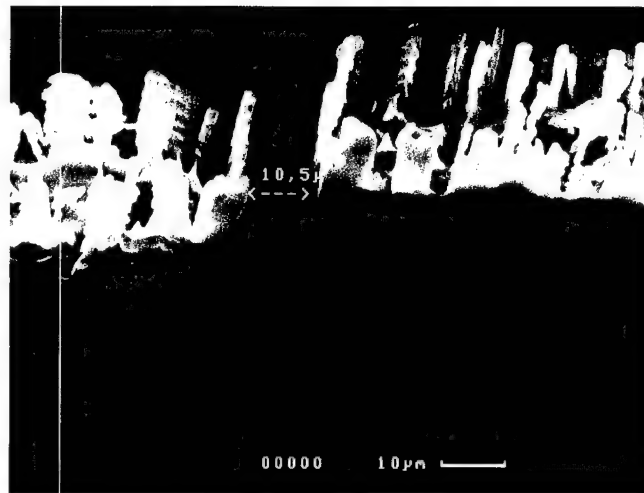


**Photo 3.** The fine structure of the gap under the electron microscope.  
Demonstration of the mask etch-off. Top-lateral view #1.

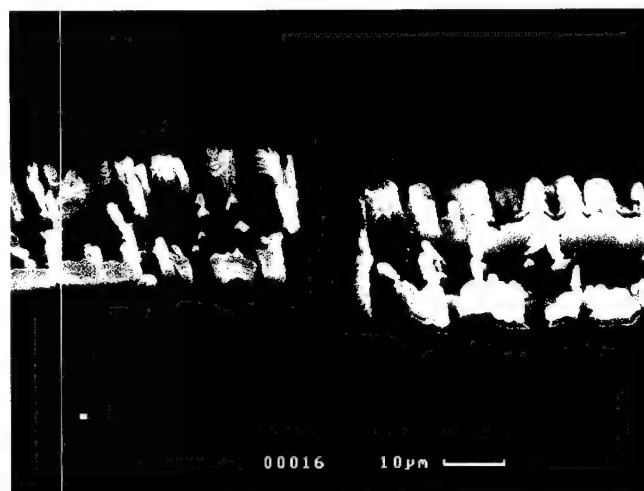


**Photo 4.** The fine structure of the gap under the electron microscope.  
Demonstration of the mask etch-off. Top-lateral view #2.

#### 4.1. MECHANICAL TESTS

The scheme of experimental set-up is shown in Fig.9. The resonance frequency of the cantilever microstructure was measured with the aid of fiber optic Fabry-Perot interferometer, in which the face of the silicon cantilever forms a Fabry-Perot cavity with the end of the optical fiber. Oscillation of the cantilever modulates the reflectivity of this cavity, so that an intensity-modulated light at the frequency of oscillation is returned by the single-mode optical fiber 1, when the cavity is illuminated with a CW laser source 2. Due to presence of directional coupler 4, about a half of the returned light propagate to the photodetector 3, which detects the modulation of the light intensity and converts this modulation into the electrical signal.

The transverse oscillation of the silicon cantilever 6 is excited by the loud-speaker 7 situated close to the micromechanical structure. The loud-speaker is powered by the low-frequency generator 9 connected to it through an amplifier 8. The generator frequency is scanned. When the amplitude of the output signal  $U_{out}$  achieves the maximum, the generator frequency corresponds to the first cantilever resonance.

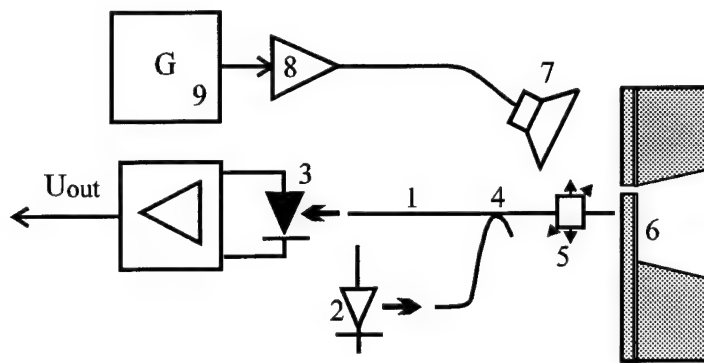


**Fig.9.** Measurement of the resonance frequency of the cantilever waveguide.

The photodetector consists of Ge-photodiode and transimpedance amplifier. It exhibited a low noise level and the uniform frequency response in the range 0-200 kHz. The laser diode with the mean optical power of 1mW and wavelength of about  $1.3\mu\text{m}$  was used as a source of the coherent radiation. The directional coupler was of X-type, fused from single-mode fibers of normal numerical aperture. At the wavelength  $\lambda=1.2915\mu\text{m}$ , which was observed at the current  $I=60\text{mA}$  and the temperature  $T=23^\circ\text{C}$ , the light propagating through the coupler was divided strictly in a half. The mean optical power in a fiber may be increased up to 2.5mW, when the current is increased to 100 mA. Interferometer created and tested by us proved to be very stable and simple in operation. The tip of the optical fiber was adjusted at the distance about several tens of microns from the cantilever waveguide. The signal-to-noise ratio of about 100 was observed.

The generator frequency was scanned in a wide range. The resonance was observed only at one frequency  $f_r=8271\text{ Hz}$ . The quality factor was measured as  $Q = f_r/\Delta f$ , where  $f_r$  is the resonance frequency, at which the amplitude of output signal  $U_{out}$  achieves the maximum value  $U_0$ , and  $\Delta f$  is the width of the resonance curve at the level  $0.7U_0$ . As a

result of this experiment the quality factor of mechanical oscillation was measured to be  $Q \approx 30$ .

#### 4.2. OPTICAL TESTS

The laboratory set-up for the optical tests of the silicon micromechanical waveguide is shown in Fig.10. The optical radiation of the laser diode 1 propagates by the single-mode optical fiber 2 coupling with the front (input) surface of the silicon waveguide 4. The position of the fiber tip is adjusted relatively the silicon structure with the aid of micropositioner 3. Propagating by the silicon waveguide 4 the light undergoes interruption at the gap. Transversal deviation of the flexible part of the waveguide gives rise to modulation of the light intensity at the rear (output) end of the silicon waveguide. This modulated light was detected by the photodiode 5 with transimpedance amplifier 6.

To adjust the optical fiber 2 with the waveguide 4 the intensity of the diode 1 was modulated with the frequency of about 20 kHz by the high-frequency generator 7. When the modulated signal appeared at the output of photodetector 5-6, the adjusting was finished and the generator 7 was switched in the cw mode.

The vibration of the cantilever was excited by the vibrating rod 8, which was set into the motion by bimorph piezoceramic 9 connected with the low-frequency generator 10. The frequency of excited vibrations was about 200 Hz.

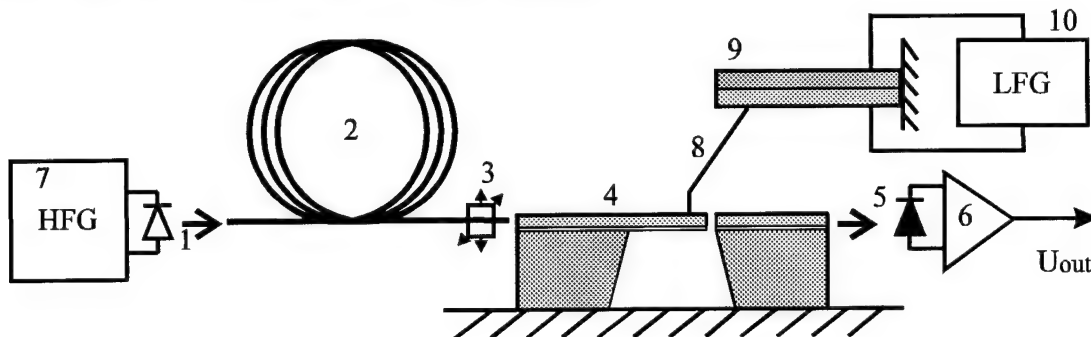


Fig.10. Scheme of the laboratory set-up for investigation of the optical properties of micromechanical silicon waveguide.

As a result of this experiment the weak modulated signal was observed at the output of the photodetector 5-6. The signal-to-noise ratio was measured to be about several units. So small amplitude of the output signal can be explained by several reasons. First, the propagating light undergoes several reflections at the surface air/silicon with 1.5db attenuation at every. Second, the silicon waveguide layer contained considerable amount of contamination (*Fe*, *Cr*, *Al*, *S*, and other elements). Third, because of strong undercutting during plasma etching, the waveguide walls were fabricated with considerable roughness, that increased the attenuation of the light propagating by the waveguide. And, finally, considerable amount of the optical power was lost at the joint between fiber 2 and the waveguide 4. In the meantime, the results obtained prove the principal feasibility of the device considered.

## 5. MECHANICAL EXCITATION OF SILICON WAVEGUIDE. THEORETICAL ANALYSIS

In our work we consider the silicon micromechanical optical waveguide in the form of the cantilever beam clamped at one end. When the cantilever is deviated, the optical waveguide is misaligned and not all the light is induced into the second part of it. This causes the modulation of the light intensity at the output of the device. To provide the light modulation it is necessary to arouse the transverse deviation of the cantilever or excite the flexural vibrations of it. There are a lot of means to excite oscillation in micromechanical waveguide or to deviate it. As an example we can name several means:

- Electrostatic excitation
- Piezoceramic excitation
- Electrothermal excitation (by integrated p-n junction, for example)
- Magnetostriction excitation
- Photothermal excitation

We shall consider in this work only excitation by direct force action, which is especially interesting for the sensor application, and photothermal and magnetostriction excitation, which were never considered before. The engineering formulas for the light intensity modulation depth  $\delta = \varepsilon/d$  (where  $\varepsilon$  is the displacement of the cantilever tip,  $d$  is the cantilever thickness) will be given for every of considered modulators.  $\delta$  is the modulation depth in static regime or at frequencies much lower than the resonance frequency. At resonance the modulation depth  $\delta_\omega$  is  $Q$  times higher, where  $Q$  is the quality factor of mechanical oscillations:  $\delta_\omega = Q\delta$ . The resonance frequency  $f_r$  of the silicon cantilever is described by the equation:

$$f_r = \frac{1.015}{2\pi} \cdot \frac{d}{l^2} \sqrt{\frac{E}{\rho}} = 1212 \frac{d}{l^2} [\text{Hz}] \quad (1)$$

where  $d$  and  $l$  are the cantilever thickness and length respectively,  $E$  is the Young's modulus and  $\rho$  is the density of silicon. The cantilever waveguide developed by us is 1 mm long and 10  $\mu\text{m}$  thick, so the resonance frequency may be estimated as 12 kHz.

The discrepancy with the experimental result for the resonance frequency may be explained by the discrepancy in the thickness of the fabricated waveguide. The thinning of the seed wafer was fulfilled by mechanical means, so the different cantilevers have the different thickness. We can find from eqn.(1) that the tested cantilever was about 7  $\mu\text{m}$  thick.

### 5.1. DIRECT FORCE ACTION

In this case the vibrating rod is acting with a force upon the cantilever beam giving rise to modulation of the light intensity. The rod may be connected with bimorph



piezoceramic and the light modulation is controlled by such a way applying the voltage to piezoceramic. This is very simple means to excite the light modulation, but it is not suitable for integration of such modulators into the microchip. On the other side this approach is very convenient for the sensor application of the device. The measured parameter (mechanical stress, acceleration, pressure, etc.) is converted into the force applied to the cantilever giving rise to modulation of the light intensity. The magnitude of the light modulation is proportional to the measured parameter.

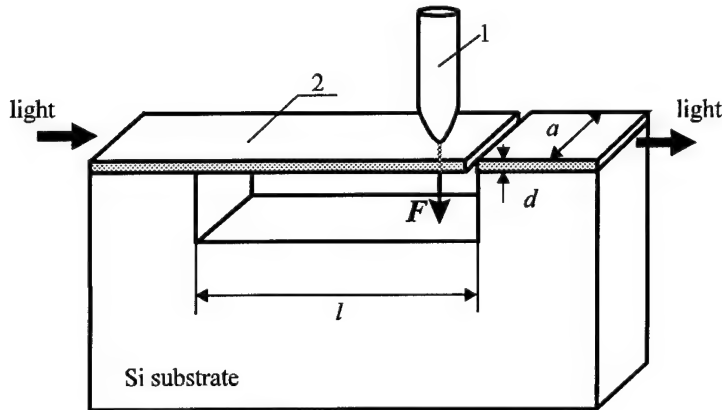


**Fig. 11.** Silicon micromechanical waveguide with direct force excitation by vibrating rod.

$F$  - applied force  
1 - vibrating rod  
2 - silicon waveguide

The modulation depth in the case of the direct force action is given by the equation:

$$\delta = \frac{4F}{E} \frac{l^3}{ad^4} \cdot 100\% \quad (2)$$

where  $F$  is the magnitude of the applied force,  $E$  is the Young's modulus of silicon cantilever,  $l$ ,  $a$ , and  $d$  are the cantilever length, width and thickness respectively.

## 5.2. PHOTOTHERMAL EXCITATION.

Another technique, which allows the light propagating by the silicon cantilever waveguide to be modulated, is photothermal excitation of waveguide oscillation [12-14]. This approach allows the light to be modulated directly by light without the use any electrical circuits and for this reason the modulator is electrically passive. The passivity means that the modulator do not distort the surrounding electric and magnetic field, do not radiate the electromagnetic waves (so its presence can not be detected) and do not sensitive to electromagnetic interferences. Passive modulators can remotely operate in the presence of strong electromagnetic interference, hostile environment, explosiveness, and at the high temperature. This conditions appear often in space, plasma, at the oil platforms, power stations, at the plain board, and in many other cases.

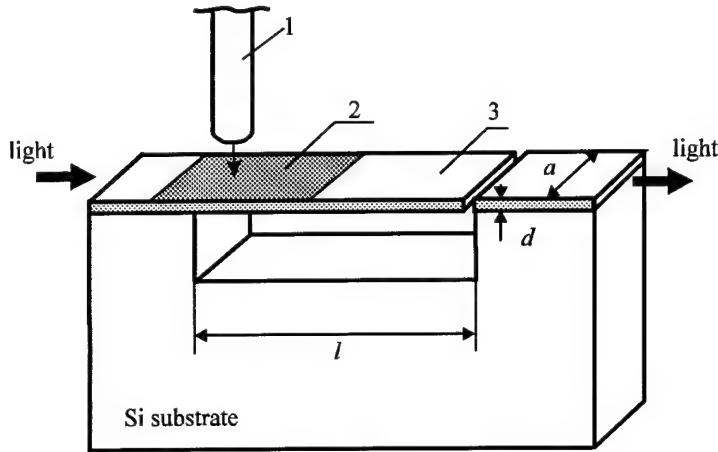


**Fig. 12.** Silicon micromechanical waveguide with photothermal excitation by modulated optical radiation

- 1 - optical fiber
- 2 - metallic coating
- 3 - silicon waveguide

Consider a modulator in the form of a rectangular cantilever with length  $l$ , width  $a$  and thickness  $d$ , coated by metal layer of thickness  $h$  (Fig.12). The following adoption were taken: the thickness  $h$  of coating is much less than the thickness  $d$  of the beam, so that we can assume that  $hE_c \ll dE_r$ . The expression for the modulation depth  $\delta$  of the silicon micromechanical optical waveguide, coated by metal from the top surface side and excited photothermally at the point of clamping by the modulated optical radiation follows:

$$\delta = 7P_\omega \frac{l^3}{ad^4} \frac{h}{d} \frac{E_c}{E_r} \frac{\alpha_c - \alpha_r}{c_0 \rho s} \cdot 100\% \quad (3)$$

where  $c_0$  is the velocity of extensional acoustic waves in silicon,  $\alpha_c$  and  $\alpha_r$  are the thermal extension coefficients of coating material and silicon respectively,  $\rho$  is the density and  $s$  is the specific heat of the silicon,  $Q$  is the quality factor of mechanical oscillation,  $E_c$  and  $E_r$  are the Young's modulus of the coating and silicon respectively,  $P_\omega$  is the mean optical power absorbed by the cantilever beam.

### 5.3. MAGNETOSTRICTION EXCITATION.

Metallic glass is well known as a material which exhibits high magnetomechanical properties such as magnetostriction and magnetomechanical coupling [15,16]. Being sputtered onto silicon waveguide the met-glass coating may serve as a drive layer giving rise to the mechanical oscillation (or static deviation) of the silicon waveguide and, consequently, to modulation of the light intensity propagating by this waveguide. For this purposes a small magnetic field should be applied along the cantilever beam, which causes the magnetostriction in the met-glass coating. Under the action of the magnetostriction the waveguide is deviated and the light intensity is modulated. In the integral chip the magnetic field necessary for the work of every modulator can be produced by a small conductive track situated near the waveguides.

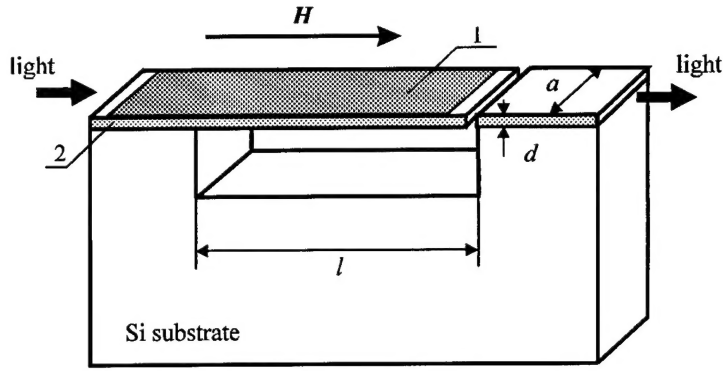


**Fig.13.** Silicon micromechanical waveguide with magnetostriction excitation by magnetic field  
*H* - magnetic field  
 1 - met-glass coating  
 2 - silicon waveguide

The calculations allow the following equation for the modulation depth  $\delta$  to be found:

$$\delta = 2\lambda_S \frac{E_{mg}}{E_{si}} \left( \frac{H_0}{H_A} \right)^2 \frac{hl^2}{d^3} \cdot 100\% \quad (4)$$

where  $E_{mg}$  and  $E_{si}$  are the Young's modulus of metallic glass and silicon respectively,  $\lambda_S$  is the magnetostriction constant,  $H_A$  is anisotropy field,  $l$  and  $d$  are the cantilever length and thickness respectively,  $h$  is the thickness of the met-glass coating,  $H_0$  is the magnitude of applied magnetic field.

For the work of such modulator the transverse domain structure should be formed in the met-glass coating. Changing the met-glass parameters the strong magnetic mechanical hysteresis can be achieved and the modulator can be used for the data storing. There are a number of means to produce the transverse domain structure. First, this is oblique sputtering of the met-glass onto silicon substrate. Second, the annealing of the device in the transverse magnetic field may be used. Third, the compressive stress may be induced into the met-glass coating giving rise to rotation of the domains. In general case this is a separate objective to develop the technology for the preparation of the met-glass magnetostrictive coating.

## 6. SENSOR APPLICATIONS OF THE DEVELOPED DEVICE

The developed modulator can be used as a sensitive element of the fiber optic sensor of force, mechanical stress, pressure, acceleration, and others force-related parameters. The main principles is that the measured parameter is converted into the force applied to the micromechanical cantilever waveguide. This force deviates the cantilever giving rise to modulation of the light propagating by the waveguide. Let us consider this opportunity on the example of the fiber optic accelerometer based on this principle.

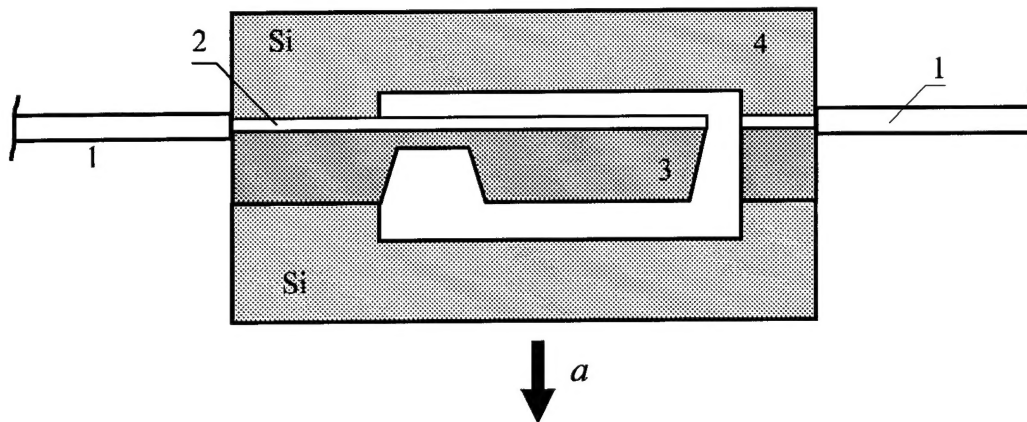


**Fig.14 . Fiber-optic accelerometer based on the silicon micromechanical optical waveguide.**

The principal scheme of the sensitive element.  $a$  is the applied acceleration.

1 - optical fiber, 2 - silicon waveguide, 3 - inertial mass, 4 - silicon encapsulation.

Fig.14 shows the principal scheme of the fiber optic accelerometer based on the silicon micromechanical optical waveguide. The inertial mass is added to the silicon cantilever to increase the sensitivity of the transducer.

## 7. RESULTS AND CONCLUSIONS

### 7.1. The results of the work:

1. The silicon micromechanical optical waveguide have been designed, fabricated, and tested.
2. Two-sides micromachining process for the device fabrication has been developed, which includes the direct silicon bonding, thinning of the seed wafer, two-side photolithography with the mask alignment in the infra-red light, anisotropic wet etching of the handle wafer, vertical dry plasma etching of the seed wafer, etc.
3. The technology for thermocompressive direct silicon bonding have been developed.
4. The technology for high-depth plasma etching has been developed. The shape of the vertical walls has been investigated with the aid of electron microscope.
5. The mechanism of photothermal and magnetostriction actuation of silicon micromechanical waveguide has been considered for the first time.
6. The photoelastic phase modulation in micromechanical waveguide has been analyzed theoretically.
7. The sensor application of the developed modulator has been considered.

### 7.2. The main conclusions:

1. Silicon optical waveguide in the form of the micromechanical cantilever clamped at one end and suspended over the square pit provides good potential for the integral cost-effective modulator/switch.
2. The direct force bending of the microbridge waveguide structure clamped at both ends calculated to be noneffective for the light modulation and the use of magnetostrictive,

piezoelectric or photothermal drive may be required in this case for the light modulation.

3. SOI waveguide structures provide the better opportunities for the micromechanical optical modulators as compared to alternative  $n/n^+$  (or  $p/p^+$ ) technique assuring fairly low propagation losses and providing more reliable and consistent fabrication process.
4. The thinning of the seed wafer by the chemical means with an etch-stop layer looks like more preferable method than the thinning by the mechanical means because of nonuniformity of the polisher/lapper (taper, bow, microrelief, variation of the pressure to the wafer, etc.).
5. The high-depth dry plasma etching requires high survivability of the metallic mask, while the shape of the walls was found to be strongly dependent upon the etch conditions: gas composition, temperature, etc. If we etch the wafer deeper than  $10\text{ }\mu\text{m}$ , the mask will be intensively etch off, while the wall may be or oblique, or curved. Several metals were tested for a mask - *Al*, *Cr*, *Ni*, *NiCr*, etc. It was experimentally found that only *Cr* and *NiCr* masks are acceptable for high-depth plasma etching. *Al* and *Ni* masks were etched off.
6. To improve the quality of the cantilever waveguide the modulator has to be designed by such a way that the thickness of the waveguide would not exceed several micrometers. In other case, there are considerable difficulties in the vertical ion-beam etching (mask etch-off, non-vertical walls and waveguide pollution). Additionally, in this case the modulator chip is as long as several millimeters.
7. The photothermal excitation of the cantilever waveguide mechanical oscillation proved to be effective enough, that allows the light to be modulated directly by light without the use any electrical circuits. The modulator built on this principles will be electrically passive and can remotely operate in the presence of strong electromagnetic interference, hostile environment, explosiveness, while its presence can not be detected electrically.
8. Being sputtered onto silicon waveguide the met-glass coating may serve as a drive layer giving rise to the mechanical oscillation (or static deviation) of the silicon waveguide and, consequently, to modulation of the light intensity propagating by this waveguide. Changing the met-glass parameters the rectangular magneto-mechanical hysteresis loop may be achieved, that allows the modulator to be used for the data storing.
9. The special grooves etched from the bottom side of the handle wafer allows the micromodulator chips to be separated by breaking, and not cutting. This simplifies the micromachining process and increases the output of good modulator chips.
10. The developed modulator can be used as a sensitive element of the fiber optic sensors of force, mechanical stress, pressure, acceleration, and others force-related parameters.

## 8. REFERENCES.

1. Soref R.A., "Silicon-based optoelectronics", 1993, *Proc. of IEEE*, v.81, No.12, pp.1687-1706
2. Soref R.A., "Silicon-Based Optical-Microwave Integrated Circuits", 1992, *Microwave Journal*, v.35, No.5, pp.230-236
3. Soref R.A., Lorenzo J.P., "All-silicon active and passive guided-wave components for 1.3 and 1.6 micrometers", *IEEE J. of Quantum Electronics*, 1986, QE-22, No.6, pp.873-879
4. Soref R.A., Cortesi E., Namavar F., Friedman L., "Vertically Integrated Silicon-on-Insulator Waveguides", *IEEE Photonics Technology Letters*, 1991, v.3, No.1, pp.22-24
5. Emmons R.M., Kurdi B.N., Hall D.G., "Buried-Oxide Silicon-on-Insulator Structures I: Optical Waveguide Characteristics", *IEEE J. of Quantum Electronics*, 1992, v.28, No.1, pp.157-163
6. T.Pirnat, L.Friedman, R.Soref, Electro-optic mode-displacement silicon light modulator, *J. Appl. Phys.*, 1991, v.70, No.6, pp.3355-3359
7. Petersen K.E., Silicon as a mechanical material, *Proc. of IEEE*, 1982, v.70, No.5, pp.420-457
8. Wilson P., "Tutorial: Silicon micro-machining", *Sensor Review*, v.10, No.4, pp.178-181, 1990
9. Pliska P., Lukosz W., "Electrically actuated nanomechanical integrated optical switches, *Proc. of the conf. on Photonics in Switching*, March 16, 1993, California, USA
10. Maszara W.P., Goetz G., Caviglia A., McKitterck J., "Bonding of silicon wafers for silicon-on-insulator", *J. Appl. Phys*, 1988., v.64, No.10, pp.4943-4950
11. Churenkov A.V., "Fabrication of Si-waveguides in <100> silicon wafer by vertical wet etching for utilization in fiber optic accelerometer", May 1992, Technical Report, University of Strathclyde, UK.
12. Langdon R.M., Lynch B.J., "Photoacoustics in optical sensors", *GEC J. of Res.*, 1988, v.6, pp.55-62
13. Optical Fiber Sensors: System and Applications, (Edited by B.Culshaw and J.Dakin), v.2, Artech House, INC.
14. Churenkov A.V., "Photothermal excitation and self-excitation of silicon microresonators", *Sensors and Actuators*, 1993, A39, pp.141-148
15. Livingston J.D., "Magnetomechanical properties of amorphous metals", *Phys. stat. sol. (a)*, 1982, v.70, p.591
16. Savage H.T., Spano M.L., Theory and application of highly magnetoelastic Metglas 2605 SC (invited), *J. Appl. Phys*, v. 53, No. 11, 1982, pp. 8092-8097